A Three-Dimensional Global Model Study of Atmospheric Methyl Chloride Budget and Distributions

Yasuko Yoshida, Yuhang Wang, Tao Zeng

School of Earth and Atmospheric Sciences, Georgia Institute of Technology

and Robert Yantosca

Division of Engineering and Applied Sciences, Harvard University

J. Geophys. Res.
In Press, 2004

Corresponding author: Yasuko Yoshida, School of Earth and Atmospheric Sciences, Georgia Institute of Technology, Atlanta, GA 30332-0340. (Email: yyoshida@eas.gatech.edu)

ABSTRACT

Global simulations of atmospheric methyl chloride (CH_3Cl) are conducted using the GEOS-CHEM model in order to understand better its sources and sinks. Observations from 7 surface sites and 9 aircraft field experiments are used to evaluate the model simulations with assimilated meteorology fields for 7 years. The model simulates CH_3Cl observations at northern mid and high latitudes reasonably well. The seasonal variation of CH_3Cl at southern mid and high latitudes is severely overestimated, however. Simulated vertical profiles of CH_3Cl are in general agreement with the observations in most regions; the disagreement occurs in the vicinities of major sources, principally reflecting the uncertainties in the estimated distributions of our added pseudo-biogenic and the biomass burning sources. Our estimate of known sources (1.5 Tg yr^{-1}) from ocean, biomass burning, incineration/industry, salt marshes, and wetlands accounts for only 34% of the total source (4.4 Tg yr^{-1}). We hypothesize that the missing source of 2.9 Tg yr^{-1} is likely of biogenic origin. On the basis of the observed CH_3Cl seasonality at northern mid and high latitudes, we find that this pseudo-biogenic source is located at 30°N–30°S, not at mid and high latitudes. If so, the observed CH_3Cl latitudinal distribution indicates that the annual hemispheric mean OH ratio is within the range of 0.8–1.3. The net uptake regions by ocean are located at high latitudes. A relatively small loss of 150 Gg yr^{-1} over these regions is critical for the model to reproduce the observed annual mean latitudinal gradient of CH_3Cl in the southern hemisphere. The large overestimate of the seasonal variation of CH_3Cl at southern mid and high latitudes likely implies that the seasonality of simulated oceanic uptake is incorrect as a result of defects in the parameterization of this loss in the model.

1. Introduction

Methyl chloride (CH_3Cl) is one of the most abundant chlorine-containing gas in the atmosphere; it is a major contributor to stratospheric chlorine. The global average mixing ratio of CH_3Cl in the troposphere is measured at about 550 ± 30 parts per trillion per volume (pptv) [*Montzka et al*., 2003]. It is believed that CH_3Cl originates in large part from natural sources [*Khalil et al.,* 1999]. According to the emission data provided in the Reactive Chlorine Emissions Inventory (RCEI) conducted under the International Global Atmospheric Chemistry (IGAC) Global Emissions Inventory Activity (GEIA) project, the estimated emissions from known sources such as biomass burning, oceans, incineration/industrial sources are 910 (650–1,120), 650 (40–950), and 162 (30–294) Gg (giga gram = 10^9 gram) yr^{-1}, respectively [*Keene et al*., 1999; *Khalil et al*., 1999; *Lobert et al*., 1999; *McCulloch et al*., 1999]. Emission from certain wood-rotting fungi is estimated at 156 (35–385) Gg yr^{-1}, though no global distribution is currently available [*Watling and Harper*, 1998; *Khalil et al*., 1999; *Lee-Taylor et al*., 2001]. In addition, *Rhew et al.* [2000] estimated annual global release of 170 (65–440) Gg of CH_3Cl from salt marshes and *Varner et al*. [1999] calculated a global flux of 48 Gg yr^{-1} from wetlands.

The major removal process of CH_3Cl in the atmosphere is due to oxidation by OH radicals, which accounts for 3.5 (2.8–4.6) Tg (tera gram = 10^{12} gram) loss per year [*Koppmann et al*., 1993]. It is estimated that about 285 Gg of tropospheric CH_3Cl is transported to the stratosphere and lost there by photo dissociation and OH oxidation. Although the ocean is a net source globally, it is a significant net local sink in high-latitude regions. The RCEI estimate for the oceanic sink over the net uptake regions is

150 Gg yr^{-1} [*Moore et al*., 1996; *Khalil et al*., 1999; *Keene et al*., 1999]. Soils are recognized as an additional sink, and *Keene et al*. [1999] estimated it could be as much as 256 Gg yr^{-1}, but the uncertainty is quite high [*Lee-Taylor et al*., 2001; *Rhew et al*. 2001]. The CH_3Cl budget based on the current "best guess" estimates given above leaves a substantial deficit for sources by ~1.8 Tg yr^{-1}. This imbalance might be explained by one or some combination of the following: (1) the emission from one or more sources is underestimated; (2) the CH_3Cl loss by reaction with OH is overestimated; (3) there exists some significant unidentified source(s) of CH_3Cl [*Keene et al*., 1999].

The overall uncertainties in CH_3Cl emissions from known sources are relatively large and the estimated OH sink has significant uncertainties that come in part from the uncertainties in the temperature dependence of the OH + CH_3Cl reaction rate constant [*Keene et al*., 1999; *Lee-Taylor et al*., 2001]. After examining the results of a series of model runs using different OH reaction rates, *Lee-Taylor et al*. [2001] concluded that the budget imbalance is not due to assumption (2) above. Their model results with identified emissions showed a significant inter-hemispheric gradient, which was not observed. In order to remove the gradient, some unidentified source must exist at high latitudes in the southern hemisphere such as oceanic emissions, which might be unrealistic considering oceanic observation results. Therefore, they concluded that the budget discrepancy likely comes from a land-based missing source [*Lee-Taylor et al*. 2001].

Yokouchi *et al*. [2000] reported that enhanced mixing ratios of CH_3Cl were correlated with α-pinene, a short-lived species emitted by vegetation, in air masses over subtropical Okinawa Island. Strong emissions of CH_3Cl from tropical plants were observed by *Yokouchi et al*. [2002] and they suggested that tropical forests could be the

major source. However, emission fluxes and the detailed emission mechanisms from terrestrial vegetation are unknown [*Keene et al*., 1999; *Yokouchi et al*., 2000; *Yokouchi et al*, 2002].

Very few global 3-D simulations of CH_3Cl have been conducted. *Lee-Taylor et al*. [2001] presented a 3-D model study for CH_3Cl distributions, but they evaluated their results using only surface observations and did not interpret the results in terms of contributions of each source to the observed concentrations and seasonal variations. In this paper we present more comprehensive modeling and analyses of CH_3Cl on the basis of surface and aircraft observations using the global GEOS-CHEM model.

2. Model description

The model used in this study is the GEOS-CHEM (version 5.02) global 3-D chemical transport model of tropospheric chemistry driven by assimilated meteorological fields from the Goddard Earth Observing System (GEOS) of the NASA Global Modeling and Assimilation Office (GMAO) (http://www-as.harvard.edu/chemistry/trop/geos/) [*Bey et al*., 2001]. We use a horizontal resolution of 4° latitude × 5° longitude. The vertical layers vary by different model simulation years. In order to compare to atmospheric field experiments, we simulated the CH_3Cl distributions using 7 different meteorological fields for the years of 1991, 1992, 1994, 1995, August 1996 – September 1997, 2000, and 2001. For simulation years before December 1995, the model has 20 vertical levels, for December 1995, 1996 and 1997, 26 levels, and for 2000 and 2001, 48 levels. To calculate the chemical loss of CH_3Cl, the tropospheric OH field was taken from the GEOS-CHEM full-chemistry simulation by *Martin et al*. [2003] and the

stratospheric OH field taken from a 2-D stratosphere/mesosphere model was used [*Schneider et al*., 2000]. The tropospheric OH field yields a global mean methyl chloroform (CH_3CCl_3) lifetime of 5.6 years in good agreement with the observations [*Spivakovsky et al*., 2000; *Prinn et al*., 2001; *Martin et al*., 2003]. In this study, CH_3Cl emitted from different sources is transported as separate tracers. In this manner, contributions from each source to the spatial and temporal distributions of CH_3Cl can be evaluated in the model.

3. Sources of CH_3Cl

Biomass burning

Biomass burning is the largest known source of CH_3Cl. *Lobert et al*. [1999] estimated 910 (650–1120) Gg yr^{-1} emissions from this source in the RCEI inventory on a $1° \times 1°$ grid based on the emission ratios of CH_3Cl to CO and CO_2. Hot spots of emission are located in the regions of Southeast Asia, India, tropical Africa and South America. No seasonality was given in the inventory; we first scaled their annual biomass burning CH_3Cl flux with seasonal biomass and biofuel burning CO emissions used in GEOS-CHEM. The satellite observation-based biomass burning CO inventory was obtained from *Duncan et al*. [2003] except for the time period of February–April 2001, when the monthly inventory by *Heald et al*. [2003] is used. Model simulations using this inventory show large overestimates over the western Pacific. *Lee-Taylor et al*. [2001] reduced the biomass burning source over Southeast Asia by 50% in the RCEI inventory. In our work, we apply a CH_3Cl/CO molar emission ratio of 5.7×10^{-4} [*Lobert et al*., 1999] to estimate a biomass burning CH_3Cl source of 611 ± 38 Gg yr^{-1}. The range reflects the interannual

variability of biomass burning CO by *Duncan et al*. [2003] and *Heald et al*. [2003]. The estimate used in our study is at the lower limit calculated by *Lobert et al*. [1999]. We found that a lower biomass burning source is in better agreement with the observations (section 5).

Oceanic emissions

The ocean is the second largest known source of CH_3Cl. In the RCEI inventory, *Khalil et al*. [1999] estimated an annual net oceanic emission of CH_3Cl of 655 Gg yr^{-1} using an empirical relationship between sea surface temperature (SST) and CH_3Cl saturation anomaly. Oceanic emissions are located mainly in the tropics and subtropics. At latitudes higher than 50°, the ocean is a net sink. The estimated uncertainties of the oceanic flux are a factor of 2 to 3, mainly due to measurement errors of several variables used in the transfer velocity calculation [*Khalil et al*., 1999]. Based on the measured solubility of CH_3Cl in seawater at different temperatures, *Moore* [2000] estimated a net CH_3Cl flux of 300–400 Gg yr^{-1} from the ocean including a global annual ocean uptake of 90–150 Gg. In this study, we recalculated the oceanic flux using the National Oceanic and Atmospheric Administration Climate Monitoring and Diagnostics Laboratory (NOAA-CMDL) empirical relationship between saturation and SST as by *Khalil et al*. [1999] with monthly climatological wind speed distributions. The wind data are taken from the revised monthly mean summaries of the Comprehensive Ocean-Atmosphere Data Set (UWM-COADS) produced at University of Wisconsin-Milwaukee in collaboration with NOAA/National Oceanographic Data Center [*daSilva et al*., 1994]. Sea surface temperature fields are the 10-year averages (1990–1999) of a global extended

reconstructed SST (ERSST) produced by *Smith and Reynolds* [2003] based on the Comprehensive Ocean-Atmosphere Data Set (COADS). The sea-air interface transfer velocity of CH_3Cl (k) was calculated following *Wanninkhof* [1992]:

$$k\ (cm\ h^{-1}) = 0.39\ v^2\ (S_c/660)^{-1/2} \quad (1)$$

$$S_c = 2385\ [1 - 0.065\ (SST) + 0.002043\ (SST)^2 - 2.6\times10^{-5}\ (SST)^3] \quad (2)$$

where v is the long-term average wind speed (m s^{-1}) at 10m above sea level, S_c is the unitless Schmidt number of CH_3Cl, and SST is in °C [*Khalil and Rasmussen*, 1999; *Khalil et al*., 1999].

In our model calculation, monthly mean sea ice coverage is applied to prevent CH_3Cl loss to the sea ice. The sea ice data are taken from the International Satellite Land-Surface Climatology Project (ISLSCP) Initiative II data archive [*Hall et al*., 2003]. Our model result of the global annual oceanic flux is about 350 Gg yr^{-1}, which is 20% lower than the value estimated by a direct extrapolation of in situ observations (440 Gg yr^{-1}) by *Khalil et al*., [1999] and 47 % lower than the 655 Gg yr^{-1} in the RCEI inventory, but is in the same range given by *Moore* [2000]. A critical issue we found in the comparison of simulated and observed surface CH_3Cl concentrations is the ocean loss over the uptake region at southern high latitudes. Our estimate of 30 Gg yr^{-1} is much lower than that in the RCEI inventory of 150 Gg yr^{-1}. Therefore, we use two inventories to account for the difference. The first inventory is as described above. In the second inventory, we increased the sink over ocean uptake regions to 150 Gg yr^{-1}. The emissions over the net source regions are increased to ~500 Gg yr^{-1} (by ~ 30%) in order to maintain the net ocean source of 350 Gg yr^{-1}.

Incineration/industrial emissions

It is known that CH_3Cl is released into the atmosphere from combustion of fossil fuels with high chlorine contents such as coal. Combustion of domestic and municipal waste containing chlorine also emits CH_3Cl. *McCulloch et al*. [1999] calculated the global emissions from fossil fuel combustion and waste incineration to be 75 ± 70 and 32 ± 23 Gg Cl yr^{-1}, respectively. They also estimated a source of 7 Gg Cl yr^{-1} from other industrial sources. The total CH_3Cl emission from coal combustion, incineration and other industrial activities is then estimated as 162 (114 ± 93) Gg yr^{-1} in the RCEI inventory [*McCulloch et al*., 1999]. In this study, we applied the non-seasonal RCEI emission inventory for this source.

Salt marshes and wetlands

Rhew et al. [2000] estimated the global CH_3Cl emissions from salt marshes as 170 (65–440) Gg yr^{-1} based on field studies from two coastal salt marshes in California. We distribute the flux using a land cover database from the International Satellite Land Surface Climatology Project (ISLSCP) Initiative I data [*Sellers et al*., 1995]. We confine the emissions to the growing season such as May to September at northern mid to high latitudes and November to March at southern mid to high latitudes.

The global CH_3Cl flux from freshwater wetlands was calculated by *Varner et al*. [1999] as 48 Gg yr^{-1}. In our model, the emissions are distributed using the ISLSCP Initiative I land cover data [*Sellers et al*., 1995] and are limited to the growing season in the same manner as in the salt marsh emission calculation.

Biogenic emissions

Close correlations between enhanced concentrations of CH_3Cl and biogenic compound, α-pinene emitted by terrestrial plants have been observed [*Yokouchi et al*., 2000]. *Yokouchi et al*. [2002] reported that some particular plant families in tropical forests (certain types of ferns and Dipterocarpaceae) emit a significant amount of CH_3Cl. They calculated that the emission from only Dipterocarpaceae species in Asian tropical forests could be 910 Gg yr^{-1} by extrapolating emission rates obtained from CH_3Cl flux measurements in a glasshouse, although the uncertainty is very large. *Hamilton et al*. [2003] estimated a global annual CH_3Cl production of 75–2,500 Gg between 30°N and 30°S based on their CH_3Cl flux observation from senescent and dead leaves. *Lee-Taylor et al*. [2001] conducted model studies for CH_3Cl, assuming that terrestrial vegetation plays a significant role in CH_3Cl production. They concluded that the model most successfully reproduced the observed mixing ratios of CH_3Cl when they added 2,330–2,430 Gg yr^{-1} of a hypothetical biogenic source combined with a 50% reduction of biomass-burning emissions from Southeast Asia in the RCEI biomass burning inventory.

In our study, 2,430–2,900 Gg yr^{-1} is added as the biogenic source of CH_3Cl. We distributed the biogenic source to all vegetated areas between 30°N and 30°S. The land cover classification is based on the ISLSCP Initiative I data set [*DeFries and Townshend*, 1994]. The uniform distribution over all vegetated areas with the flat annual emission rate is based on model sensitivity analyses (the results are not shown) since currently the dependence of biogenic CH_3Cl emission on vegetation, temperature, and sunlight is unknown. The major constraint is the observed seasonal variation of CH_3Cl at northern mid and high latitudes. Biogenic emissions at mid and high latitudes in summer would

lead to overestimates of CH_3Cl in those regions. Furthermore, scaling biogenic CH_3Cl emission to the seasonality of isoprene (e.g., *Lee-Taylor et al*., [2001]) would also lead to a too small seasonal variation in comparison to the observations because the seasonality of isoprene emissions is opposite to the observed seasonality of CH_3Cl. Our calculated emissions between 30°S–30°N account for 93% of the global CH_3Cl source, which agrees with the estimates by *Khalil and Rasmussen* [1999], who suggested that 85% of the emission of CH_3Cl comes from tropical and subtropical regions based on their inverse modeling results with simplified box models for tropospheric transport and OH oxidation.

4. Sinks of CH_3Cl

Reaction with OH

The main sink of CH_3Cl in the atmosphere is oxidation by hydroxyl radicals:

$$CH_3Cl + OH \rightarrow CH_2Cl + H_2O \qquad (R1)$$

In our model calculation, we used two different reaction rate constants for reaction (R1), k_{97}, and k_{03}, reported by *DeMore et al*. [1997] and *Sander et al*. [2003], respectively. The rate constant (k) is represented by the Arrhenius expression $k = A \exp(-E/RT)$, where values for A given by *DeMore et al*. [1997] and *Sander et al*. [2003] are 4.0×10^{-12} and 2.4×10^{-12} cm^3s^{-1}, and for E/R, 1400 and 1250K, respectively. T is temperature (K). The rate constant at 298K is 3.6×10^{-14} cm^3s^{-1} for both, and the uncertainty (at 298K) is 1.2 and 1.15, respectively. The k_{03} is higher than k_{97} by about 9% at T=250K. The calculated global losses of CH_3Cl with the "reference" emissions (Table 1) using k_{97} and k_{03} are 4.1 Tg yr^{-1} for both, which agree with literature values [*Koppmann et al*., 1993; *Khalil and*

Rasmussen, 1999]. The model results with the different k value are compared in section 5.1.

The OH field used is taken from the work by *Martin et al*. [2003]. The interhemispheric ratio of mass-weighted OH is 1.03; about 2.6% higher in the northern hemisphere (NH) than in the southern hemisphere (SH). Calculated annual mean global CH_3CCl_3 lifetime to loss by tropospheric OH is 5.6 years, which is consistent with estimates from observations by *Spivakovsky et al*. [2000] (5.7 ± 0.7 years) and *Prinn et al*. [2001] (6.0 +1.0, –0.7 years). However, the interhemispheric OH ratio calculated from CH_3CCl_3 measurements using the inverse method varies by study. For instance, the NH/SH ratio estimated by *Prinn et al*. [2001] and *Krol and Lelieveld* [2003] is 0.88 and 0.98, respectively. *Krol and Lelieveld* [2003] commented that the differences between their interhemispheric ratio and that given by *Prinn et al*. [2001] could be due to the model resolution difference. They also explained that their slightly higher OH concentrations in the SH than NH might be derived from model or emission errors. Nearly equal hemispheric mean OH was also reported by *Spivakovsky et al.* [2000].

In order to test the sensitivity of the CH_3Cl distribution to reaction with OH in our model, we conducted three test simulations using OH fields with different NH/SH distribution, such as original OH field (the annual mean NH/SH mass ratio is 1.03), OH increased and decreased by 10% (NH/SH ratio of 1.26), and decreased and increased by 10% (NH/SH ratio of 0.84), in the NH and SH, respectively. Figure 1 shows the resulting latitudinal CH_3Cl distributions with different OH distributions compared with observed concentrations. In these simulations, the reaction rate constant was taken from *Sander et al*. [2003]. The result with the original OH concentrations gives almost symmetrical N-S

distribution as observed while results with modified OH fields show clear N-S gradients. It is therefore clear that deviation from the current hemispheric mean OH ratio by ±20% could not reproduce the observed CH_3Cl distributions. The additional constraint on the interhemispheric mean OH ratio is valuable because the estimate is not as sensitive to model errors of the interhemispheric transport as that derived from CH_3CCl_3, the source of which is located in the northern industrial regions.

Soil sink

The global soil sink of CH_3Cl is estimated to be 256 Gg yr^{-1} [*Keene et al*., 1999; *Khalil and Rasmussen*, 1999]. No global distribution of the soil uptake rates is available. *Rhew et al*. [2001] found that there is a strong correlation in the measured uptake rates of CH_3Br and CH_3Cl in southern California shrubland ecosystems, and concluded there could be a similar mechanism of consumption for both compounds. In our model, we scaled the soil sink of CH_3Cl with that of methyl bromide (CH_3Br), whose global loss rates were estimated by *Shorter et al*. [1995], assuming that the soil uptake of CH_3Cl is proportional to CH_3Br. The soil type was defined using vegetation type data from the ISLSCP Initiative I data [*DeFries and Townshend*, 1994]. Seasonality was applied by assuming growing seasons of 365, 240, and 180 days in tropical, temperate, and boreal regions, respectively [*Shorter et al*., 1995]. The calculated annual CH_3Cl loss to soil is, 69, 137, 16, and 34 Gg yr^{-1} for tropical forest/savanna, temperate forest/grassland, boreal forest, and cultivated land, respectively.

5. Results

We conducted several model runs with different input data: one of them employs the sources from existing emission inventories such as the RCEI inventories (for oceanic, biomass burning, incineration/industrial sources) and pseudo-biogenic emission of the literature value (i.e., *Lee-Taylor et al*. [2001]), which is referred to as the reference run. Run OC-1 includes the oceanic and biomass burning emissions calculated in our model (section 3). The oceanic sink in run OC-1 is about 80% smaller than that calculated by *Khalil et al*. [1999] and it resulted in higher average surface concentrations in the SH by about 10 pptv (~2%) than in the NH, which is not observed. In run OC-2, oceanic emissions and sinks are increased so that total oceanic sink over net uptake regions becomes the same as that given by RCEI [*Khalil et al*. 1999] and the net oceanic emissions are the same as in OC-1 run. The runs of reference, OC-1 and OC-2 are simulated with the same meteorological field of September 1996–August 1997. Figure 2 summarizes the latitudinal distribution of the annual-mean emissions and sinks (except the sink via OH oxidation) of CH_3Cl used in those runs. The average values of 7-year model runs (1991, 1992, 1994, 1995, Sep96–Aug97, 2000, 2001) are shown as "model mean". The annual total of the emissions and sinks are listed in Table 1. Figure 3 shows simulated global surface CH_3Cl mixing ratio distributions for January and July. Higher concentrations are simulated over regions where major sources are located. The lower concentrations in the summer hemisphere are due in part to active OH oxidation.

The model results are evaluated with surface and aircraft observations. Seven surface sites and 9 aircraft field experiments are included. Table 2 summarizes these observations used.

5.1. Global distribution of atmospheric CH_3Cl near the surface

5.1.1 Seasonal variation

Our model results are compared with three surface observation data sets measured at 7 surface stations. The locations of these 7 sites are shown in Figure 4. The observed and simulated seasonal variations of CH_3Cl at the stations are compared in Figure 5. The data from *Khalil and Rasmussen* [1999] was lowered by 8.3% in all figures in order to adjust to the calibration difference [*Montzka et al*., 2003]. We note that the CMDL data may have a systematic error up to 20 pptv due to losses of CH_3Cl in field deployed reference tanks (*G. Dutton*, personal communication, 2004). There are two observed data sets for Alaska, Hawaii, Samoa, Tasmania and Antarctica, and those two seasonal variations are similar except in Samoa, where the CMDL data show two peaks in February–March and in August, while a single peak in June–July was reported by *Khalil and Rasmussen* [1999].

The model results with a total emission of 4,500 Gg yr^{-1} ("reference" in Table 1) with different OH reaction rate constants (k_{97} and k_{03}, section 4) are shown in Figure 5 as Ref-k97 and Ref-k03, respectively. The other model results shown as OC-1, OC-2, and model mean are calculated using k_{03}. The global annual mean surface concentration of Ref-k97 and Ref-k03 is 599 and 579 pptv, respectively, and the difference, about 3%, is solely due to the difference of the reaction rate constants. The reference run with k_{97} (Ref_k97) gives higher concentrations than the observations by 3–18% especially at the tropical and NH sites. Using the rate constant k_{03}, the run Ref-k03 overestimates the observations by up to 14% except for January–June at Tasmania and Antarctica sites. For these two sites, the OC-2 concentrations are close to the Ref-k03 concentrations except

for June–October in Tasmania, where Ref-k03 gives lower concentrations by 3–4%. The overestimates of Ref-k03 indicate that the biomass burning emissions in the RCEI inventory might be overestimated. The wrong seasonality simulated in the Ref-k03 run is due to the scaling of the biogenic source to isoprene emissions, which peak in summer, when observed CH_3Cl shows a minimum.

OC-1 and OC-2 show little difference at all sites except for Tasmania and Antarctica, where the effect of the oceanic uptake of CH_3Cl is significant. OC-2 gives lower concentrations than OC-1 by about 2–5% in better agreement with the observations. The model results with our estimates of biomass burning and oceanic emissions with increased oceanic sink over the uptake regions (OC-2 and Model mean) reproduces the general features and the magnitudes of seasonal variations relatively well at northern high latitude stations (Alaska, Ireland and Oregon), such as maxima in spring to early summer and minima in late summer and fall. At the Hawaii site, the summer overestimate is largest in August in Ref-k97. The peak for the multi-year mean is not as large, but the summer overestimate is apparent, suggesting that the biogenic source upwind from Hawaii is overestimated. The amplitude of the seasonal cycle calculated by the model is too large compared to the observations at southern higher latitudes. The reasons will be discussed further in the next section.

5.1.2. Latitudinal variation

Figure 6 shows the annual and seasonal latitudinal distributions of CH_3Cl at the same 7 surface stations in Figure 4. The observed annual means of CH_3Cl show little interhemispheric gradient, while there are relatively clear seasonal gradients. Ref-k03

overestimates the observations in the tropics and northern higher latitudes. A possible reason for the higher concentrations in the NH for the run Ref-k03 is that the biomass burning emissions are biased towards the NH. The estimated NH/SH ratio of biomass burning emissions by *Lobert et al*. [1999] is about 2.2; whereas we calculated a ratio of 1.6 based on scaling to the biomass burning CO inventory [*Duncan et al*., 2003]. *Lee-Taylor et al*. [2001] mentioned that they reduced the biomass burning CH_3Cl flux from southern and eastern Asia by half in order to reduce the interhemispheric gradient in their model results. The overestimates of Ref-k03 at low latitudes could be explained by the distribution of the isoprene-scaled biogenic emissions, which are biased toward equatorial regions (Figure 2).

The difference between OC-1 and OC-2 runs shows the effect of oceanic sink on surface concentrations. These two runs have almost the same net oceanic emissions, but OC-2 has more than four-times the oceanic sink over the net uptake regions than OC-1. Since the SH has more oceanic area than the NH, the concentrations of CH_3Cl are more sensitive to ocean uptake in the SH than the NH. The OC-1 run shows a south-north gradient while OC-2 shows a symmetrical distribution as observed (Figure 6-a). However, the simulated seasonal variations in OC-2 and for other years ("model mean") are much higher than the observations. It largely reflects the small seasonal variation in the ocean uptake at southern high latitudes, which is ±2 Gg yr^{-1} as compared to ±100 Gg yr^{-1} driven by the seasonality of the OH chemistry. The physical parameterization is based on wind speed and SST [*Khalil et al*., 1999]. *Khalil et al*. [1999] mentioned that this proxy calculation represented the flux for warm waters well, but not the uptake in cold waters. *Tokarczyk et al*. [2003] reported that the CH_3Cl degradation rate constants

have no clear SST dependence. Further investigation is needed to understand the mechanisms controlling the seasonality of ocean uptake.

5.2. Vertical profiles of atmospheric CH_3Cl

Figure 7 shows the vertical distributions of CH_3Cl from aircraft measurements and our model for regions shown in Figure 4. Model results are taken from simulations with assimilated meteorology for the same period as the observations except for PEM-Tropic B and INDOEX, for which the GMAO assimilated meteorological data for GEOS-CHEM are unavailable. For these two missions, we use the average of 7-year runs for 1991, 1992, 1994, 1995, Sep1996–Aug1997, 2000 and 2001. The OC-2 oceanic sink of uptake regions is applied. The contribution for individual sources is shown. We discuss the results by geographical region.

Tropical Pacific (PEM-Tropics A and B)

The PEM-Tropics A took place over the remote South Pacific Ocean between August 24 and October 6, 1996. The observations of CH_3Cl show little variation with altitude except over the eastern Pacific region (ep) (Figures 7-1 – 7-4). Over this region, the observations show elevated concentrations at about 2–4 km, which reflects the easterly outflow of air masses from South America that were strongly influenced by biomass burning emissions [*Blake et al*., 1999a]. The model closely reproduces the observations for Fiji (fj) although it overestimates for the eastern Pacific region (ep) especially near the surface, where concentrations are over-predicted due to biogenic

CH_3Cl emissions from tropical rain forests in our model (Figure 7-4). For Hawaii (hwi), the model concentrations are higher than the observations by ~30 pptv for all altitudes.

Measurements during the PEM-Tropics B mission were taken over the tropical Pacific in March and early April 1999. Observed and simulated values are compared for Fiji (fj) and Tahiti (tht) regions (Figure 7-5, 7-6). The model simulations generally show slight overestimates. *Blake et al*. [2001] reported that CH_3Cl concentrations observed in PEM-Tropics A were higher than observed in PEM-Tropics B south of 10°S because of significant biomass burning emissions during PEM-Tropics A in the tropical dry season. In Figures 7-1 –7-6, however, this trend is not obvious in regional profiles because we average the concentrations over larger areas as shown in Figure 4. The latitude-altitude plots discussed in section 5.3 (Figures 8-1, 8-2, 8-5 and 8-6) show this trend.

Tropical Pacific and Southern Oceans (ACE 1)

The ACE 1 mission was conducted over the Pacific and Southern Oceans during November and December 1995. Slight positive vertical gradients of CH_3Cl were observed for samples taken over the four regions shown in Figure 4 (Figures 7-7 – 7-10). *Blake et al*. [1995b] explained the vertical trend could be derived from the long range transport of air containing high biomass burning CH_3Cl. Our model results overestimate the concentrations for all regions except the Tasmania-December region (tas-dec). Simulated CH_3Cl also shows greater vertical gradients for all regions except for the Tahiti-November region (tht-nov). The overestimates of the vertical gradient in the model are mainly due to our pseudo-biogenic CH_3Cl rather than biomass burning CH_3Cl.

Tropical Atlantic (TRACE-A)

The TRACE-A mission, in September–October 1992, focused on investigating the effects of biomass burning over the South Atlantic, South America, and southern Africa. The observed enhancements of CH_3Cl in the boundary layer (at 0–2 km) over Brazil/South America (sa) and southern Africa (af) (Figures 7-11 and 7-13) indicate the regional biomass burning effects [*Blake et al*., 1996]. Over South America, another maximum was observed above 10 km. Analyzing samples collected at high altitude and the boundary layer, *Blake et al*. [1996] concluded that biomass burning over Brazil and frequent deep convection within and downwind of the fires could explain the enhanced concentrations in the upper troposphere. The model reproduces the maxima in the boundary layer observed over South America and southern Africa, while it underestimates the magnitudes. In addition to the biomass burning source suggested by *Blake et al*. [1996], our model indicates that our added biogenic source contributes significantly to the boundary layer enhancement (Figures 7-11 and 7-13). The biomass burning source of CH_3Cl is often deduced by the enhancement ratio of CH_3Cl to CO on the basis of field measurements. Our model results suggest that such deduced biomass burning source of CH_3Cl could be overestimated if the biogenic contribution to the observed CH_3Cl to CO enhancements ratios is not properly accounted for.

The model does not reproduce the observed high concentrations in the upper troposphere over South America (Figure 7-11). However, no such large enhancement is evident over the tropical South Atlantic (Figure 7-12) or Africa (Figure 7-13). The convective enhancement at 12 km may therefore reflect the biased sampling of specific convective plumes by the DC-8 aircraft, which would not be reflected in the simulated

monthly mean concentrations. Over the South Atlantic (oc) (Figure 7-12), the vertical profile of measured CH_3Cl concentrations shows slight increases with altitude and the model matches relatively well with the observations except at 0–2 km, where combined biogenic and biomass burning CH_3Cl concentrations result in a maximum that was not present in the observations.

Indian Ocean (INDOEX)

During the INDOEX campaign air samples were collected over the northern Indian Ocean in February–March 1999. Enhanced concentrations of CH_3Cl and other combustion tracers such as CO, hydrocarbons, and CH_3CN were observed in the outflow from India and Southeast Asia, indicating that extensive biofuel emissions in those areas contributed to the high CH_3Cl levels [*Scheeren et al*., 2002]. The model underestimates the observations at all altitudes (Figure 7-14). Based on the INDOEX observations, *Scheeren et al*. [2002] reported a CH_3Cl/CO molar emission ratio of 1.74×10^{-3} for the biofuel emissions, which is about three times larger than that of 0.57×10^{-3} [*Lobert et al*., 1999] used in our model. Increasing the biofuel CH_3Cl/CO molar ratio to 1.74×10^{-3} led to an increase of 50 pptv in India and Southeast Asia, resulting in a better agreement with the observations (not shown).

Western Pacific (PEM-West A and B, TRACE-P)

The PEM-West A mission was conducted in September and October 1991 over the western Pacific. During the PEM-West B mission, air samples were collected from February to March 1994. One major feature in the vertical profiles of CH_3Cl during

PEM-West A (Figure 7-15 – 7-17) is the enhanced concentrations observed at high altitude (above 10 km), which reflect transport of CH_3Cl by typhoons [*Blake et al*., 1997; *Kondo et al*., 1997; *Newell et al*., 1996]. The model results show little vertical variation and did not reproduce those elevated concentrations. Higher CH_3Cl mixing ratios observed below 6 km during PEM-West B than PEM-West A in the southwest (sw) region (Figures 7-16, 19) could be explained by stronger westerly outflow from the Asian continent in winter than in fall [*Blake et al*., 1997; *Kondo et al*., 1997]. During PEM-West B, little vertical variations were observed over Guam (gm) and Japan (jp) (Figures 7-18, 20), reflecting small influence from the continental outflow while over the southwest (sw) region, CH_3Cl concentrations are higher at 0–5 km (Figure 7-19). Our model tends to overestimate the observations possibly as the result of its tendency to transport too much biogenic CH_3Cl from low latitudes. In the southwestern region, simulated concentrations show some enhancements at low altitude (~3 km), which are due to biogenic and biomass burning emissions (Figure 7-19).

The measurements during TRACE-P were obtained over the northwestern Pacific between February and April 2001. During this mission, a strong influence of Asian outflow was detected, which also characterized the main feature of the PEM-West B observations [*Jacob et al*., 2003]. TRACE-P observations indicate significant effects of biomass burning emissions at high altitudes [*Liu et al*., 2003; *Russo et al*., 2003]. In the eastern region of TRACE-P (e), our model results show higher concentrations at middle altitudes than observed; the model bulge is largely attributed to the biogenic source (Figure 7-21). In the western region (w), both the model and observed (mean) values are higher in the boundary layer and decrease with altitude, reflecting higher concentrations

of incineration/industrial and biomass burning sources near the surface (Figure 7-22). The simulated CH_3Cl concentrations from the biosphere appear to be overestimated. We will examine the potential causes of the overestimates in the next section.

North America (TOPSE)

The TOPSE experiment was carried out during February to May 2000 at mid to high latitudes over North America. Figures 7-23 – 7-30 show monthly mean observed and simulated vertical profiles for northern and southern TOPSE regions in Figure 4. Slight positive vertical gradients were observed throughout the measurement period. The largest vertical gradients were observed at mid latitudes in February and March (Figures 7-23, 24). Our model closely reproduces the observed concentrations in general. However, it does not reproduce the higher vertical gradients in February and March due to the overestimated emissions near the surface. The positive vertical gradients are largely attributed by the model to biogenic CH_3Cl transported from the tropics.

5.3. Latitude-altitude distribution of atmospheric CH_3Cl

Latitude-altitude cross sections of observed and simulated CH_3Cl concentrations for selected aircraft field experiments are compared in Figure 8. Figure 9 illustrates the relative difference between observed and simulated values. During PEM-Tropics A, a slight north-south gradient was observed over the Tahiti region; the concentrations south of 10°S are higher by about 20 pptv than in the northern section. Our model simulates the observations well for the southern section, where the difference is within ±5%, but overestimates by 5 to 15% in the northern section (Figures 8-2, 9-2). Simulated surface

concentrations are too high due to the westward transport of model biogenic and biomass burning CH_3Cl from Central and South America. Unfortunately, there are not enough data points to see the latitudinal variability for the other three PEM-Tropics A regions, though Figures 9-2 – 9-4 show that the model tends to overestimate the concentrations close to the equator near the surface, resulting mainly from the strong outflow of biogenic CH_3Cl mentioned above.

During PEM-Tropics B, the concentration gradient observed over the Fiji region is opposite of that during PEM-Tropics A (Figure 8-5). The model captures the trend although it overestimates the concentrations by ~10% for some locations (Figure 9-5). The simulated latitudinal gradient is due to the combination of biomass burning and biogenic CH_3Cl gradients in the model. There are not enough data points to investigate the spatial variability for TRACE-A.

During PEM-West B, the model overestimates the observations by 5 to 20% in most regions (Figure 9-10). A few "hot spots" (670–750 pptv) were observed in the lower troposphere around 10°N that could be attributed to biomass burning plumes [*Blake et al*., 1997]; they are shifted to the northern latitudes in the model results (Figure 8-10). After investigating the correlation of CH_3Cl with CO during PEM-West B, *Blake et al*. [1997] concluded that at latitudes north of 25°N, no significant amount of CH_3Cl is emitted from urban/industrial sources or from other high-latitude continental sources and that the enhanced concentrations observed at low latitudes (<25°N) could result from the continental biomass burning outflow. The high concentrations simulated in the model near 25°N are due to biomass burning and biogenic emissions.

Figure 8-11 shows a comparison of observed and simulated spatial variability for the TRACE-P experiment. The enhanced concentrations observed in the boundary layer north of 25°N were due to fossil fuel/biofuel combustion effluent from China. During TRACE-P, transport of biomass burning effluents from Southeast Asia was limited to high altitudes south of 35°N [*Blake et al*., 2003b; *Liu et al*., 2003]. The model reproduces the general trend, but shows a more distinct latitudinal gradient. The model overestimates the observations at 20°–30°N by 5–15% as a result of strong model transport of biogenic CH_3Cl descending from the upper troposphere (Figure 9-11). This strong subsidence persists at the same location, even when the biogenic emissions are restricted to 10°S to 10°N in the model (results not shown), indicating stronger influence of transport from the tropics on mid-latitude CH_3Cl concentrations in the model than is apparent from the observations. Simulated concentrations at 0–2 km north of 30°N are lower by <5% than the observed values. Considering the strong boundary layer Asian outflow at 30°–45°N during TRACE-P [*Liu et al*., 2003], incineration/industrial and/or biofuel emissions in our model could be underestimated.

Figures 9-12 – 9-15 show the difference between the observations and model simulations for the TOPSE experiment. The model closely reproduces the observations. Spatial variations and their seasonal evolution of CH_3Cl concentrations are shown in Figures 8-12 – 8-15. Higher concentrations were observed in the middle troposphere at lower latitudes (<60°N). The latitudinal/altitudinal concentration gradient decreases with season reflecting the reduction of CH_3Cl transport from the tropical regions. The model reproduces the seasonal trend properly. The higher concentrations in the middle

troposphere might be explained by CH_3Cl transport from biomass burning and biogenic sources from the tropics and Southeast Asia.

6. Conclusions

We apply a global 3-D chemical transport model, GEOS-CHEM, to simulate the global distributions of CH_3Cl. The model simulations are constrained by surface and aircraft observations to define better the characteristics of the required pseudo-biogenic source of atmospheric CH_3Cl that we added to the model and to examine the observational constraints on the other better-known sources. Contributions from the pseudo-biogenic, oceanic, biomass burning, incineration/industrial, salt marsh and wetland sources are quantified through tagged-tracer simulations. Their effects on seasonal variations, latitudinal trends, and regional vertical profiles of CH_3Cl are investigated.

We find that a pseudo-biogenic source of 2.9 Tg yr^{-1} (66% of the total source) is necessary to explain the observed CH_3Cl concentrations. The large decrease of CH_3Cl from summer to winter at northern mid latitudes implies a negligible biogenic source of CH_3Cl at mid latitudes. We therefore constrain the pseudo-biogenic emissions to 30°S–30°N. Furthermore, we find that scaling the pseudo-biogenic emission to that of isoprene [e.g., *Lee-Taylor et al*., 2001] leads to an underestimate of the seasonal CH_3Cl variation at northern mid latitudes and tends to concentrate CH_3Cl to a few tropical and subtropical ecosystems resulting in overestimates of aircraft observations downwind from these regions. We assume that tropical and subtropical ecosystems have the same aseasonal

emission rate, which gives better simulations of the observations than scaling the emissions to those of isoprene.

Our model mean annual CH_3Cl oceanic flux over the net emission regions is 510 Gg yr^{-1}, 37% smaller than the RCEI inventory [*Khalil et al*. 1999]. The calculated total oceanic sink over the uptake regions is about 30 Gg yr^{-1}, which is about one fifth of the RCEI inventory [*Khalil et al*., 1999]. We find that the ocean uptake plays an important role in reproducing the observed annual-mean latitudinal gradient of CH_3Cl at southern high latitudes, where the uptake is significant. Increasing the oceanic sink over the uptake regions to 150 Gg yr^{-1}, which is the same as in the RCEI inventory, results in the model reproducing well the observed annual-mean latitudinal gradient of CH_3Cl. Our model overestimates the seasonal variation of CH_3Cl at southern mid and high latitudes, implying an underestimate of the seasonal variation of ocean uptake calculated based on SST and wind speed.

Our calculated CH_3Cl emission from the biomass/biofuel burning source using a molar CH_3Cl/CO emission ratio of 5.7×10^{-4} is 610 Gg yr^{-1}, which is about two thirds of that given in RCEI inventory [*Lobert et al*., 1999]. Our lower biomass burning CH_3Cl emissions yield better agreement with the observed symmetrical annual-mean latitudinal CH_3Cl gradient, while the model results using biomass burning source data from the RCEI inventory show a clear bias towards overestimates in the northern hemisphere.

Our estimated total emission of CH_3Cl from six sources including our 2.9 Tg yr^{-1} pseudo-biogenic source and the other identified sources such as biomass/biofuel burning, ocean, incineration/industry, salt marshes, and wetlands in the model is approximately 4.4 Tg yr^{-1}. The calculated atmospheric burden of CH_3Cl is about 5.0 Tg and the

estimated tropospheric lifetime of CH_3Cl against OH oxidation is about 1.2 years. The interhemispheric symmetry in the latitudinal distribution of CH_3Cl and a dominant tropical/subtropical pseudo-biogenic source imply that the annual hemispheric mean OH ratio is constrained to the range of 0.8–1.3.

A major shortfall in our current understanding of CH_3Cl emissions is the geographical distributions of the biogenic and biomass burning sources. This uncertainty is reflected clearly in the model comparison with aircraft observations. The model simulates generally well vertical profiles of CH_3Cl in most regions especially for high latitudes, where there is little local emission, while the model tends to overestimate or underestimate the observations near biogenic and biomass burning sources, reflecting the uncertainties in those source distributions. The model overestimates the observations over the western Pacific due to the simulated influx of biogenic CH_3Cl associated with the strong subsidence at 20°–30°N. It is noteworthy that the model suggests the dominant source of CH_3Cl in the region is biogenic, while previous studies focused mostly on biomass burning emissions [e.g., *Blake et al*., 1997; *Liu et al*., 2003; *Russo et al*., 2003]. Biomass burning emission sources are likely overestimated in those studies although large uncertainty of the estimated biogenic CH_3Cl source needs to be considered. The comparison over the tropical regions suggests that the model biogenic sources in Central and South America might be overestimated. The estimates of CH_3Cl over India and Southeast Asia suggest that the CH_3Cl/CO molar emission ratio in this region is higher than the value we used in the model. Applying a single CH_3Cl/CO emission ratio to the globe is too simplistic since the CH_3Cl emission rate depends on the fuel type and the

burning conditions [*Lobert et al*, 1999]. The estimated incineration/industrial or biofuel emissions near the coast of China might be underestimated.

Acknowledgments. We thank David Erickson and Jose L. Hernandez for providing us the UWM-COADS data and helpful comments. We thank Donald Blake for his suggestions. We thank Derek Cunnold for providing us the AGAGE data. We are grateful to CMDL and Geoff Dutton for providing us their unpublished data. We also thank Daniel Jacob and Colette Heald for their help. The GEOS-CHEM model is managed at Harvard University with support from the NASA Atmospheric Chemistry Modeling and Analysis Program. This work was supported by the NASA ACMAP program.

References

Bey, I., D. J. Jacob, R. M. Yantosca, J. A. Logan, B. Field, A. M. Fiore, Q. Li, H. Liu, L. J. Mickley, and M. Schultz, Global modeling of tropospheric chemistry with assimilated meteorology: Model description and evaluation, *J. Geophys. Res*., 106, 23,073 – 23,096, 2001.

Blake, N.J., D. R. Blake, O., B. C. Sive, T-Y. Chen, F. S. Rowland, J. E. Collins Jr., G. W. Sachse, and B. E. Anderson, Biomass burning emissions and vertical distribution of atmospheric methyl halides and other reduced carbon gases in the South Atlantic region, *J. Geophys. Res*., 101, 24,151 – 24,164, 1996.

Blake, N.J., D. R. Blake, O., T-Y. Chen, J. E. Collins Jr., G. W. Sachse, B. E. Anderson, and F. S. Rowland, Distribution and seasonality of selected hydrocarbons and halocarbons over the western Pacific basin during PEM-West A and PEM West B, *J. Geophys. Res*., 102, 28,315 – 38,331, 1997.

Blake, N.J., D. R. Blake, O. W. Wingenter, B. C. Sive, L. M. McKenzie, J. P. Lopez, I. J. Simpson, H. E. Fuelberg, G. W. Sachse, B. E. Anderson, G. L. Gregory, M. A. Carroll, G. M. Albercook, and F. S. Rowland, Influence of southern hemispheric biomass burning on midtropospheric distributions of nonmethane hydrocarbons and selected halocarbons over the remote South Pacific, *J. Geophys. Res*., 104, 16,213 – 16,232, 1999a.

Blake, N.J., D. R. Blake, O., O. W. Wingenter, B. C. Sive, C. H. Kang, D. C. Thornton, A. R. Bandy, E. Atlas, F. Flocke, J. M. Harris, and F. S. Rowland, Aircraft measurements of the latitudinal, vertical, and seasonal variations of NMHCs, methyl

nitrate, methyl halides, and DMS during the First Aerosol Characterization Experiment (ACE 1), *J. Geophys. Res*., 104, 21,803 – 21,817, 1999b.

Blake, N.J., D. R. Blake, I. J. Simpson, J. P. Lopez, N. A. Johnston, A. L. Swanson, A. S. Katzenstein, S. Meinardi, B. C. Sive, J. J. Colman, E. Atlas, F. Flocke, S. A. Vay, M. A. Avery, and F. S. Rowland, Large-scale latitudinal and vertical distributions of NMHCs and selected halocarbons in the troposphere over the Pacific Ocean during the March-April 1999 Pacific Exploratory Mission (PEM-Tropics B), *J. Geophys. Res*., 106, 32,627 – 32,644, 2001.

Blake, N.J., D. R. Blake, B. C. Sive, A. S. Katzenstein, S. Meinardi, O. W. Wingenter, E. L. Atlas, F. Flocke, B. A. Ridley, and F. S. Rowland, The seasonal evolution of NMHCs and light alkyl nitrates at middle to high northern latitudes during TOPSE, *J. Geophys. Res*., 108, 8359, doi:10.1029/2001JD001467, 2003a.

Blake, N.J., D. R. Blake, I. J. Simpson, S. Meinardi, A. L. Swanson, J. P. Lopez, A. S. Katzenstein, B. Barletta, T. Shirai, E. Atlas, G. Sachse, M. Avery, S. Vay, H. E. Fuelberg, C. M. Kiley, K. Kita, and F. S. Rowland, NMHCs and halocarbons in Asian continental outflow during the Transport and Chemical Evolution over the Pacific (TRACE-P) field campaign: Comparison with PEM-West B, *J. Geophys. Res*., 108, 8806, doi:10.1029/2002JD003367, 2003b.

daSilva, A., A. C. Young, and S. Levitus, Atlas of Surface Marine Data 1994, Volume 1: Algorithms and Procedures, *Tech. Rep. 6,* U.S. Department of Commerce, NOAA, NESDIS,, 1994.

DeFries, R. S. and J. R. G. Townshend, NDVI-derived land cover classification at global scales, *Int. J. Remote Sensing*, 15, 3567 – 3586, 1994.

DeMore, W. B., S. P. Sander, D. M. Golden, R. F. Hampson, M. J. Kurylo, C. J. Howard, A. R. Ravishankara, C. E. Kolb, and M. J. Molina, Chemical kinetics and photochemical data for use in stratospheric modeling, *JPL Publ. 97-4, Eval.,12*, Jet Propul. Lab., Pasadena, Calif., 1997.

Duncan, B. N., R. V. Martin, A. C. Staudt, R. Yevich, and J. A. Logan, Interannual and seasonal variability of biomass burning emissions constrained by satellite observations, *J. Geophys. Res.*, 108, 4040, doi:10.1029/2002JD002378, 2003.

Guenther, A., C. N. Hewitt, D. Erickson, R. Fall, C. Geron, T. Graedel, P. Harley, L Klinger, M. Lerdau, W. A, Mckay, T Pierce, B. Scholes, R. Steinbrecher, R. Tallamraju, J. Taylor, and P. Zimmerman, A global model of natural volatile organic compound emissions, *J. Geophys. Res*., 100, 8873 – 8892, 1995.

Hall, F. G., B. Meeson, S. Los, L. Steyaert, E. Brown de Colstoun, and D. Landis, eds. ISLSCP Initiative II. NASA. DVD/CD-ROM. NASA, 2003.

Hamilton, J. T. G., W. C. McRoberts, F. Keppler, R. M. Kalin and D. B. Harper, Chloride methylation by plant pectin: an efficient environmentally significant process, *Science*, 301, 206 – 209, 2003.

Heald, C. L., D. J. Jacob, P. I. Palmer, M. J. Evans, G. W. Sachse, H. B. Singh, and D. R. Blake, Biomass burning emission inventory with daily resolution: application to aircraft observation of Asian outflow, *J. Geophys. Res*., 108, 8368, doi: 10.1029/2002JD002732, 2003.

Jacob, D. J., B. D. Field, E. M. Jin, I. Bey, Q. B. Li, J. A. Logan, R. M. Yantosca, and H. B. Singh, Atmospheric budget of acetone, *J. Geophys. Res*., 107, art. no. 4100, May 2002.

Jacob, D. J., J. H. Crawford, M. M. Kleb, V. S. Connors, R. J. Bendura, J. L. Raper, G. W. Sachse, J. C. Gille, L. Emmons, and C. L. Heald, Transport and chemical evolution over the Pacific (TRACE-P) aircraft mission: design, execution, and first results, *J. Geophys. Res*., 108, 9000, doi:10.1029/2002JD003276, 2003.

Keene, W. C., M. A. K. Khalil, D. J. Erickson III, A. McCulloch, T. E. Graedel, J. M. Lobert, M. L. Aucott, S. L. Gong, D. B. Harper, G. Kleiman, P. Midgley, R. M. Moore, C. Seuzaret, W. T. Sturges, C. M. Benkovitz, V. Koropalov, L. A. Barrie, and Y. F. Li, Composite global emissions of reactive chlorine from anthropogenic and natural sources: Reactive Chlorine Emissions Inventory, *J. Geophys. Res*., 104, 8429 – 8440, 1999.

Khalil, M. A. K., and R. A. Rasmussen, Atmospheric methyl chloride, *Atmos. Environ*., 33, 1305 – 1321, 1999.

Khalil, M .A. K., R. M. Moore, D. B. Harper, J. M. Lobert, D. J. Erickson, V. Koropalov, W. T. Sturges, and W. C. Keene, Natural emissions of chlorine-containing gases: Reactive Chlorine Emissions Inventory, *J. Geophys. Res*., 104, 8333 – 8346, 1999.

Kondo, Y., M. Koike, S. Kawakami, H. B. Singh, H. Nakajima, G. L. Gregory, D. R. Blake, G. W. Sachse, J. T. Merrill, and R. E. Newell, Profiles and partitioning of reactive nitrogen over the Pacific Ocean in winter and early spring, *J. Geophys. Res*., 102, 28,405 – 28,424, 1997.

Koppmann, R., F. J. Johnen, D. Plass-Dülmer, and J.Rudolph, Distribution of methyl chloride, dichloromethane, trichloroethene and tetrachloroethene over the North and South Atlantic, *J. Geophys. Res*., 98, 20,517 – 20,526, 1993.

Krol, M., and J. Lelieveld, Can the variability in tropospheric OH be deduced from measurements of 1,1,1-trichloroethane (methyl chloroform)?, *J. Geophys. Res*., 108, 4125, doi:10.1029/2002JD002423, 2003.

Lee-Taylor, J. M., G. P. Brasseur, and Y. Yokouchi, A preliminary three-dimensional global model study of atmospheric methyl chloride distributions, *J. Geophys. Res*., 106, 34,221 – 34,233, 2001.

Liu, H., D. J. Jacob, I. Bey, R. M. Yantosca, B. N. Duncan, and G. W. Sachse, Transport pathways for Asian pollution outflow over the Pacific: Interannual and seasonal variations, *J. Geophys. Res*., 108, 8786, doi:10.1029/2002JD003102, 2003.

Lobert, J. M., W. C. Keene, J. A. Logan and R. Yevich, Global chlorine emissions from biomass burning: Reactive Chlorine Emissions Inventory, *J. Geophys. Res*., 104, 8373 – 8389, 1999.

Martin, R. V., D. J. Jacob, R. M. Yantosca, M. Chin, and P. Ginoux, Global and regional decreases in tropospheric oxidants from photochemical effects of aerosols, *J. Geophys. Res*., 108, 4097, doi: 10.1029/2002JD002622, 2003.

McCulloch, A., M. L. Aucott, C. M. Benkovitz, T. E. Graedel, G. Kleiman, P. M. Midgley, and Y. F. Li, Global emissions of hydrogen chloride and chloromethane from coal combustion, incineration and industrial activities: Reactive Chlorine Emissions Inventory, *J. Geophys. Res*., 104, 8391 – 8403, 1999.

Montzka, S. A., P. J. Fraser (lead authors),J. H. Butler, P. S. Connell, D. M. Cunnold, J. S. Daniel, R. G. Derwent, S. Lal, A. McCulloch, D. E. Oram, C. E. Reeves, E. Sanhueza, L. P. Steele, G. J. M. Velders, R. F. Weiss, R. J. Zander, Controlled substances and other source gases, Chapter 1 in *Scientific Assessment of Ozone*

Depletion: 2002, Global Ozone Research and Monitoring Project—Report No. 47, World Meteorological Organization, Geneva, 2003.

Moore, R. M., The solubility of a suite of low molecular weight organochlorine compounds in seawater and implications for estimating the marine source of methyl chloride to the atmosphere, *Chemosphere: Global Change Science*, 2, 95 – 99, 2000.

Moore, R. M., W. Groszko, and S. J. Niven, Ocean-atmosphere exchange of methyl chloride: Results from NW Atlantic and Pacific Ocean studies, *J. Geophys. Res*., 101, 28,529 – 28,538, 1996.

Newell, R. E., W. Hu, Z-X. Wu, Y. Zu, H. Akimoto, B. E, Anderson, E. V. Browell, G. L. Gregory, G. W. Sachse, M. C. Shipham, A. S. Bachmeier, A. R. Bandy, D. C. Thornton, D. R. Blake, F. S. Rowland, J. D. Bradshaw, J. H. Crawford, D. D. Davis, S. T. Sandholm, W. Brockett, L. DeGreef, D. Lewis, D. McCormick, E. Monitz, J. E. Collins Jr., B. G. Heikes, J. T. Merrill, K. K. Kelly, S. C. Liu, Y. Kondo, M. Koike, C.-M. Liu, F. Sakamaki, H. B. Singh, J. E. Dibb, and R. W. Talbot, Atmospheric sampling of Supertyphoon Mireille with NASA DC-8 aircraft on September 27, 1991, during PEM-West A, *J. Geophys. Res*., 101, 1853 – 1871, 1996.

Prinn, R. G., J. Huang, R. F. Weiss, D. M. Cunnold, P. J. Fraser, P. G. Simmonds, A. McCulloch, C. Harth, P. Salameh, S. O'Doherty, R. H. J. Wang, L. Porter, B. R. Miller, Evidence for substantial variations of atmospheric hydroxyl radicals in the past two decades, *Science*, 292, 1882 – 1888, 2001.

Rhew, R. C., B. R. Miller, and R. F. Weiss, Natural methyl bromide and methyl chloride emissions from coastal salt marshes, *Nature*, 403, 292 – 295, 2000.

Rhew, R. C., B. R. Miller, M. K. Vollmer, and R. F. Weiss, Shrubland fluxes of methyl bromide and methyl chloride, *J. Geophys. Res*., 106, 20,875 – 20,882, 2001.

Russo, R. S., R. W. Talbot, J. E. Dibb, E. Scheuer, G. Seid, D. E. Jordan, H. E. Fuelberg, G. W. Sachse, M. A. Avery, S. A. Vay, D. R. Blake, N. J. Blake, E. Atlas, A. Fried, S. T. Sandholm, D. Tan, H. B. Singh, J. Snow, and B. G. Heikes, *J. Geophys. Res*., 108, 8804, doi:10.1029/2002JD003184, 2003.

Sander, S. P., A. R. Ravishankara, D. M. Golden, C. E. Kolb, M. J. Kurylo, M.J. Molina, G. K. Moortgat, and B. J. Finlayson-Pitts, Chemical kinetics and photochemical data for use in stratospheric modeling, *JPL Publ. 02-25, Eval.,14*, Jet Propul. Lab., Pasadena, Calif., 2003.

Scheeren, H. A., J. Lelieveld, J. A. de Gouw, C. van der Veen, and H. Fischer, Methyl chloride and other chlorocarbons in polluted air during INDOEX, *J. Geophys. Res*., 107, 8015, doi:10.1029/2001JD001121, 2002.

Schneider, H. R., D. B. A. Jones, M. B. McElroy, and G.-Y. Shi, Analysis of residual mean transport in the stratosphere: 1. Model description and comparison with satellite data, *J. Geophys. Res*., 105, 19,991 – 20,011, 2000.

Sellers, P. J., S. O. Los, C. J. Tucker, C. O. Justice, D. A. Dazlich, G. J. Collatz, and D. A. Randall, A global 1 by 1 degree NDVI data set for climate studies. Part 2: The generation of global fields of terrestrial biophysical parameters from the NDVI, *International Journal of Remote Sensing*, 15(17), 3519 – 3545, 1994.

Sellers, P. J., B. W. Meeson, F. G. Hall, G. Asrar, R. E. Murphy, R. A. Schiffer, F. P. Bretherton, R. E. Dickinson, R. G. Ellingson, C. B. Field, K. F. Huemmrich, C. O. Justice, J. M. Melack, N. T. Roulet, D. S. Schimel, and P. D. Try, Remote sensing of

the land surface for studies of global change: Models - algorithms – experiments, *Remote Sens. Environ*., 51(1), 3 – 26, 1995.

Sellers, P. J., S. O. Los, C. J. Tucker, C. O. Justice, D. A. Dazlich, G. J. Collatz, and D. A. Randall, A revised land surface parameterization (SiB2) for atmospheric GCMs. Part 2: The generation of global fields of terrestrial biophysical parameters from satellite data, *Journal of Climate,* 9(4), 706 –737, 1996.

Shorter, J. H., C. E. Kolb, P. M. Crill, R. A. Kerwin, R. W. Talbot, M. E. Hines, and R. C. Harriss, Rapid degradation of atmospheric methyl bromide in soils, *Nature*, 377, 717 – 719, 1995.

Simmonds, P. G., S. O'Doherty, R. G. Derwent, A. J. Manning, D. B. Ryall, P. Fraser, L. Porter, P. Krummel, R. Weiss, B. Miller, P. Salameh, D. Cunnold, R. Wang, and R. Prinn, In-situ AGAGE observations by GC-MS of methyl bromide and methyl chloride at the Mace Head, Ireland and Cape Grim, Tasmania (1998-2001) and their interpretation, submitted to *J. Atmos. Chem*., 2004

Smith, T. M. and R. W. Reynolds, Extended reconstruction of global sea surface temperature based on COADS data (1854-1997), *Journal of Climate*, 16, 1495 –1510, 2003.

Spivakovsky, C. M., J. A. Logan., S. A. Montzka, Y. J. Balkanski, M. Foreman-Fowler, D. B. A. Jones, L. W. Horowitz, A. C. Fusco, C. A. M. Brenninkmeijer, M. J. Prather, S. C. Wofsy, and M. B. McElroy, Three-dimensional climatological distribution of tropospheric OH: Update and evaluation, *J. Geophys. Res*., 105, 8391 – 8980, 2000.

Talbot, R. W., J. D. Bradshaw, S T. Sandholm, S. Smyth, D. R. Blake, N. R. Blake, G. W. Sachse, J. E. Collins, B. G. Heikes, B. E. Anderson, G. L. Gregory, H. B. Singh,

B. L. Lefer, and A. S. Bachmeier, Chemical characteristics of continental outflow over the tropical South Atlantic Ocean from Brasil and Africa, *J. Geophys. Res*., 101, 24,187 – 24,202, 1996.

Tokarczyk, R., K. D. Goodwin, and E. S. Saltzman, Methyl chloride and methyl bromide degradation in the Southern Ocean, *Geophys. Res. Lett*., ,30, 1808, doi:10.1029/2003GL017459, 2003.

Varner, R. K., P. M. Crill, and R. W. Talbot, Wetlands: a potentially significant source of atmospheric methyl bromide and methyl chloride, *Geophys. Res. Lett*.,26, 2433 – 2436, 1999.

Wanninkhof, R., Relationship between wind speed and gas exchange over the ocean, *J. Geophys. Res*., 97, 7373 – 7382, 1992.

Watling, R., and D. B. Harper, Chloromethane production by wood-rotting fungi and an estimate of the global flux to the atmosphere, *Mycol.Res*., 102, 769 – 787, 1998.

Yokouchi, Y., Y. Noijiri, L. A. Barrie, D. Toom-Sauntry, T. Machida, Y. Inuzuka, H. Akimoto, H.-J. Li, Y. Fujinuma, and S. Aoki, A strong source of methyl chloride to the atmosphere from tropical coastal land, *Nature,* 403, 295 – 298, 2000.

Yokouchi, Y., M. Ikeda, Y. Inuzuka, and T. Yukawa, Strong emission of methyl chloride from tropical plants, *Nature,* 416, 163 – 165, 2002.

Table 1. Estimated global budget of CH_3Cl

Unit: Gg yr^{-1}

Runs	Reference	OC-1	OC-2	Model mean
SOURCES (total)	**(4,525)**	**(4,214)**	**(4,333)**	**(4,399 ± 43)**
Ocean	805[a]	380	499	508 ± 5
Biomass burning	910[b]	554	554	611 ± 38
Incineration/industrial	162[c]	162[c]	162[c]	162[c]
Pseudo biogenic	2,430[d]	2,900	2,900	2,900
Salt marshes	170[e]	170[e]	170[e]	170[e]
Wetlands	48[f]	48[f]	48[f]	48[f]
SINKS (total)	**(4,525)**	**(4,214)**	**(4,333)**	**(4,399 ± 43)**
OH reaction	4,124	3,926	3,930	3,994 ± 42
Ocean	145[a]	32	147	149 ± 1
Soil	256[g]	256[g]	256[g]	256[g]

[a - g] Those values are taken from the following references: [a] *Khalil et al*. [1999], [b] *Lobert et al*. [1999], [c] *McCulloch et al*. [1999], [d] *Lee-Taylor et al*. [2001], [e] *Rhew et al*. [1999], [f] *Varner et al*. [1999], [g] *Khalil and Rasmussen* [1999] and *Keene et al*. [1999]. Other emissions and sinks are calculated as explained in the text.

Table 2. Atmospheric measurements of CH_3Cl

	Region	Time period	Reference
Surface stations			
K & R	Alaska (71.2N, 156.5W) Oregon (45.5N, 124W) Hawaii (19.3N, 154.5W) Samoa (14.1S, 170.6W) Tasmania (42S, 145E) Antarctica (90S)	1981-1997	*Khalil and Rasmussen* [1999]
NOAA-CMDL	Alaska (71.3N, 156.6W) Hawaii (19.5N, 155.6W) Samoa (14.2S, 170.6W) Antarctica (90.0S, 102.0E)	Jan 1998-Mar 2002 Dec 1999-Feb 2002 Dec 1998-Feb 2003 Jan 2001-Nov 2003	*G. Dutton, personal communication,* 2004
AGAGE	Ireland (53.2N, 9.5W) Tasmania (40.4S, 144.4E)	1998-2001	*Simmonds et al*. [2004]
Aircraft missions			
PEM-Tropics A	Tropical Pacific	Aug-Oct 1996	*Blake et al*. [1999a]
PEM-Tropics B	Tropical Pacific	Mar-Apr 1999	*Blake et al*. [2001]
ACE 1	Pacific/Southern Ocean	Nov-Dec 1995	*Blake et al*. [1999b]
TRACE-A	Tropical Atlantic	Sep-Oct 1992	*Blake et al*. [1996]
INDOEX	Indian Ocean	Feb-Mar 1999	*Scheeren et al*. [2002]
PEM-West A	Western Pacific	Sep-Oct 1991	*Blake et al*. [1997]
PEM-West B	Western Pacific	Feb-Mar 1994	*Blake et al*. [1997]
TRACE-P	Western Pacific	Feb-Apr 2001	*Blake et al*. [2003b]
TOPSE	North America	Feb-May 2000	*Blake et al*. [2003a]

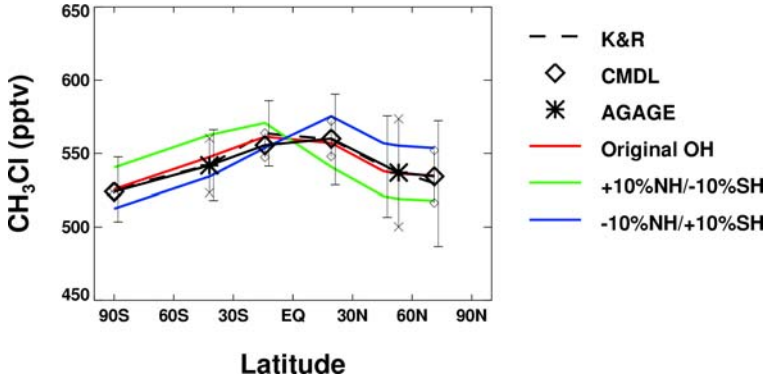

Figure 1. Latitudinal distributions of observed and simulated CH_3Cl at the surface sites. Broken line indicates data by *Khalil and Rasmussen* [1999] (the data were lowered by 8.3% to account for a calibration difference). The thick black solid line links the CMDL (Diamonds) and AGAGE data (asterisks). Thin vertical lines indicate the standard deviations; the end symbols are minus signs, diamonds, and asterisks for K&R, CMDL, and AGAGE data, respectively. Emission inventories for OC-2 (Table 1) are used. Model results are shown with the standard OH concentrations and two perturbation cases, in which the NH and SH hemispheric OH concentrations are either increased or decreased by 10% (see text for more details).

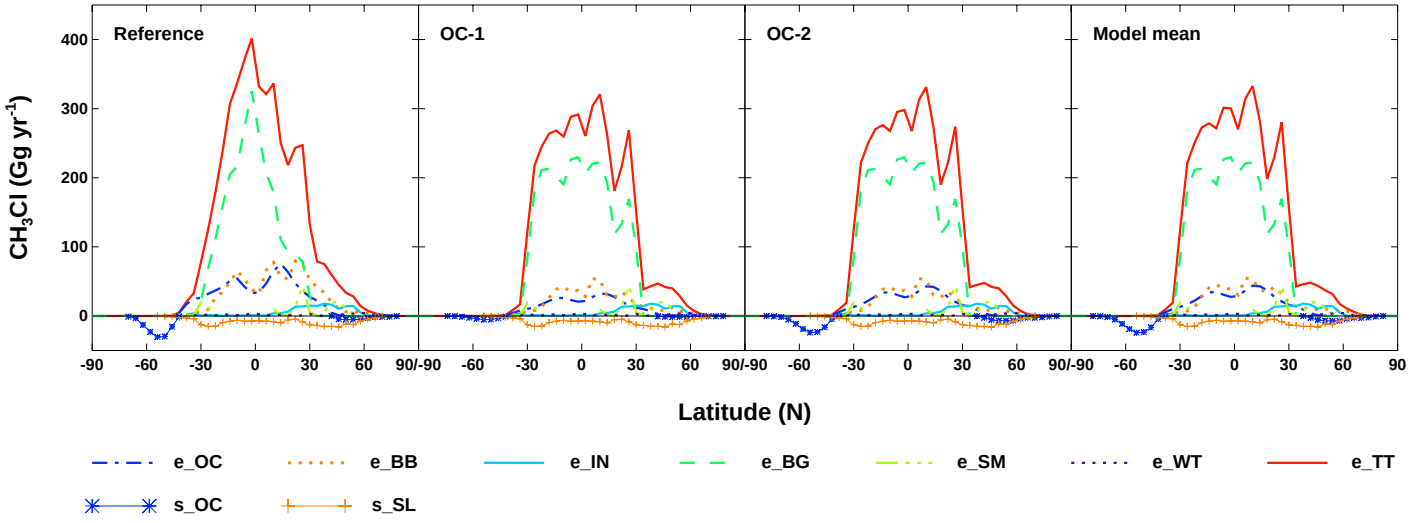

Figure 2. Latitudinal distribution of the known sources and sinks of CH_3Cl. For the legend, "e-" and "s-" denote emission and sink, respectively and characters OC, BB, IN, BG, SM, WT, TT, SL denote ocean, biomass burning, incineration/industrial, biogenic, salt marshes, wetlands, the total of all emissions, and soil, respectively.

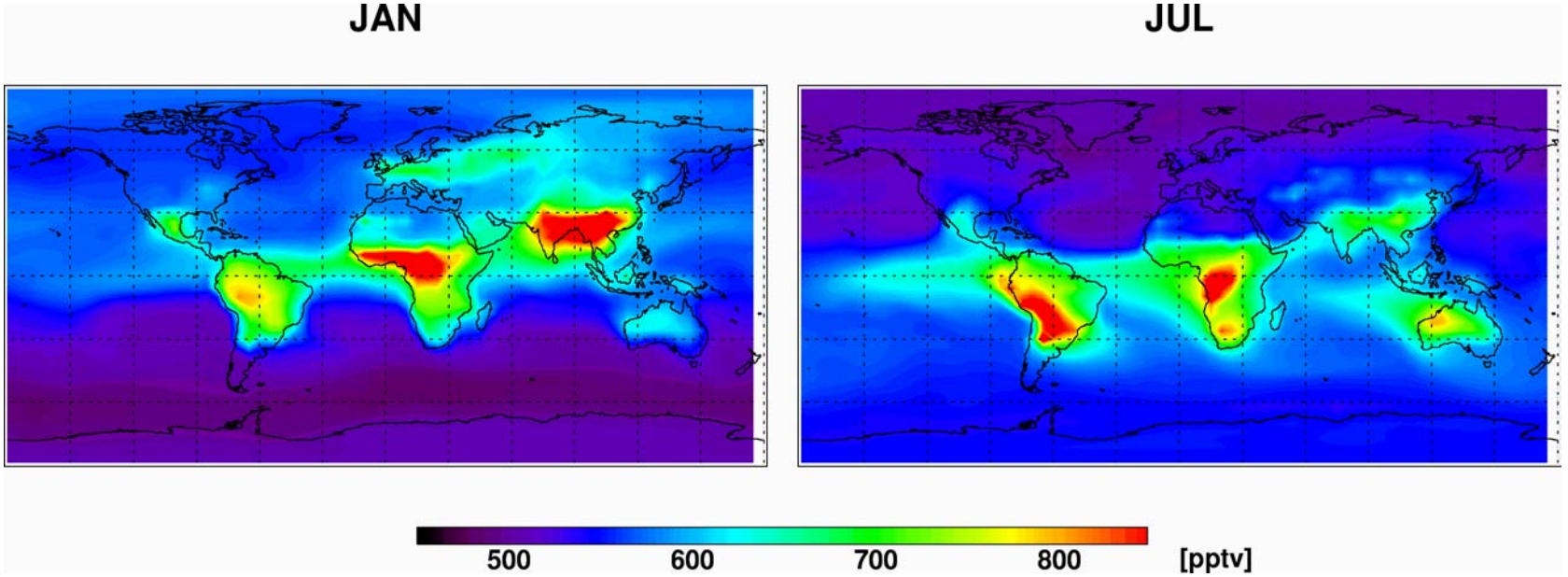

Figure 3. Simulated surface mixing ratio of CH_3Cl for January and July.

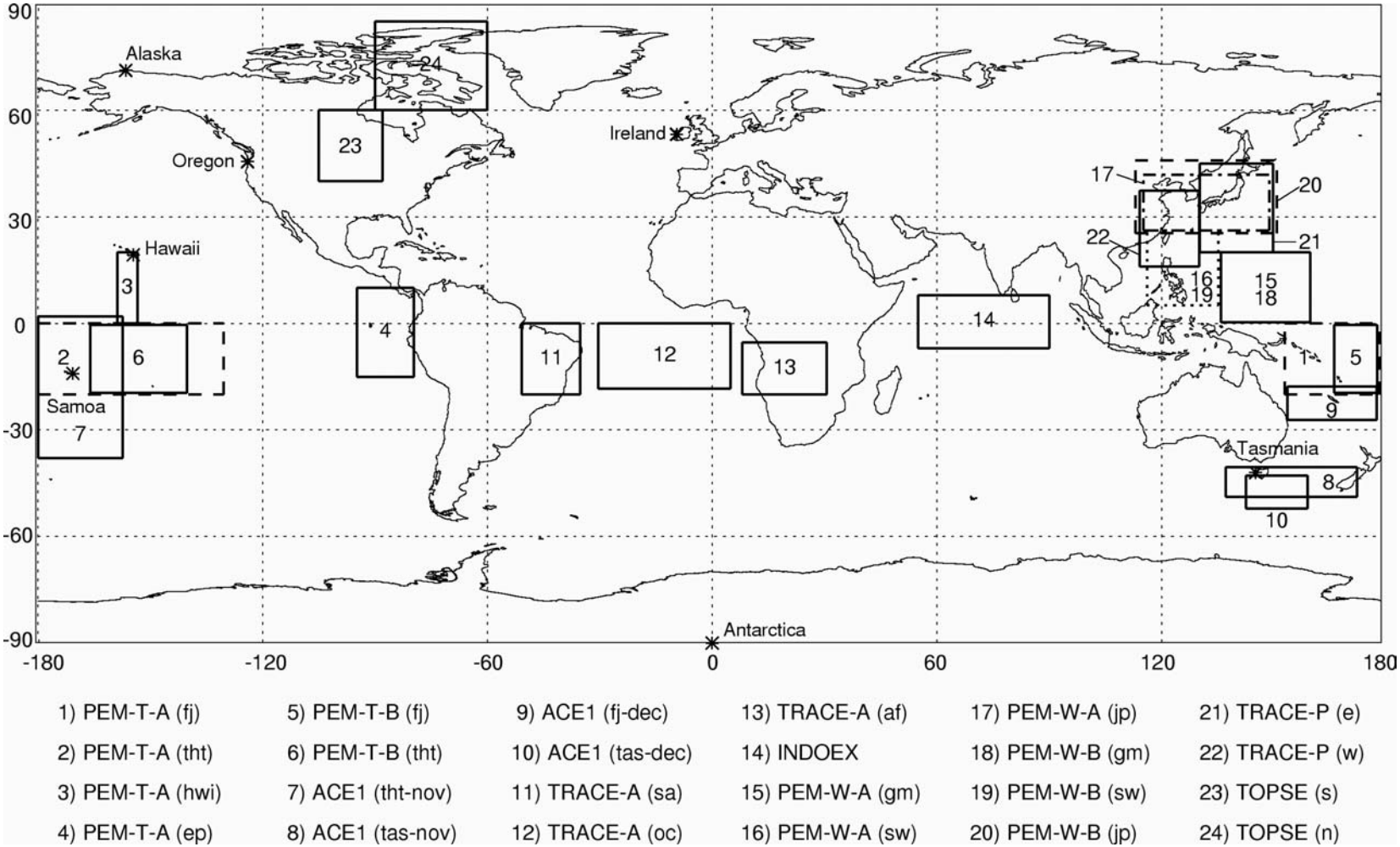

Figure 4. Surface measurement sites (indicated by symbols) and aircraft observation regions used in this study.

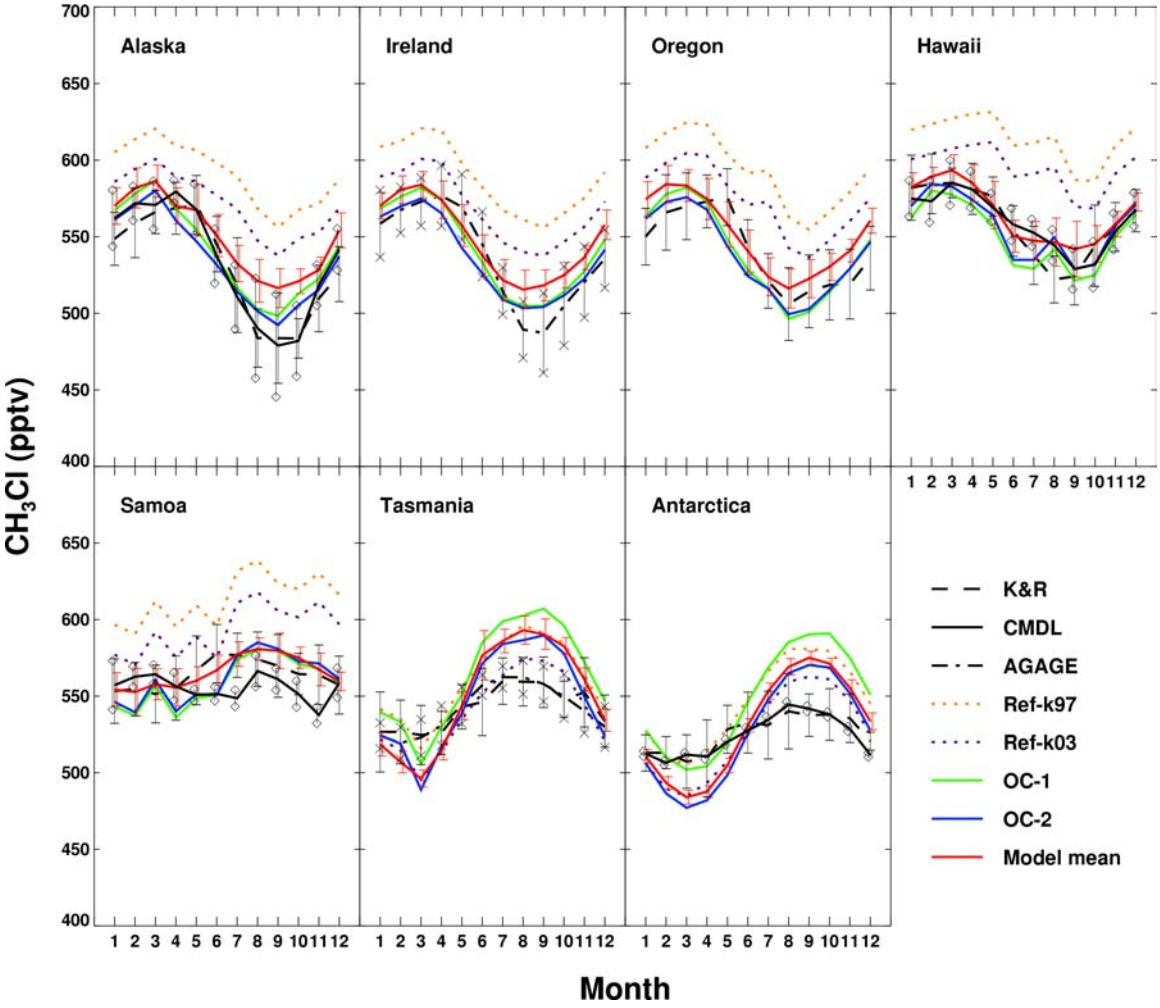

Figure 5. Seasonal variations of observed and simulated CH_3Cl at the surface sites. Broken lines indicate data by *Khalil and Rasmussen* [1999], black solid lines indicate CMDL data (G. *Dutton*, personal communications, 2004), and dotted-broken lines indicate AGAGE data [*Simmonds et al*., 2004]. The K&R data were lowered by 8.3% to account for a calibration difference. Model results are shown in color. The orange dotted lines are the reference run with the OH reaction rate constant by *DeMore et al*. [1997]. The purple dotted lines are the reference run with the OH rate constant by *Sander et al*. [2003]. The green lines are the OC-1 run. The blue lines are the OC-2 run. These 4 simulations used meteorological data for September 1996 – August 1997. The red solid lines are the mean of 6-year simulations with oceanic sink calculated as in the OC-2 run. The vertical lines represent the standard deviations.

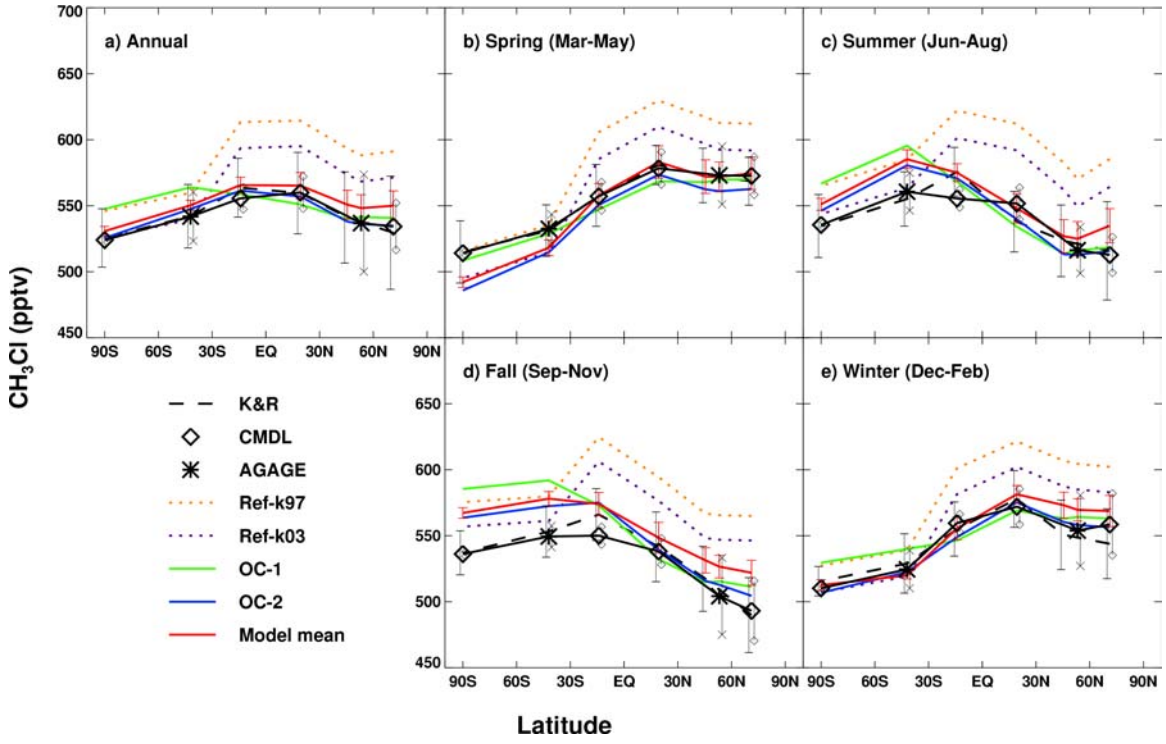

Figure 6. Latitudinal distributions of observed and simulated CH_3Cl at the surface sites. Line symbols are the same as Figure 5.

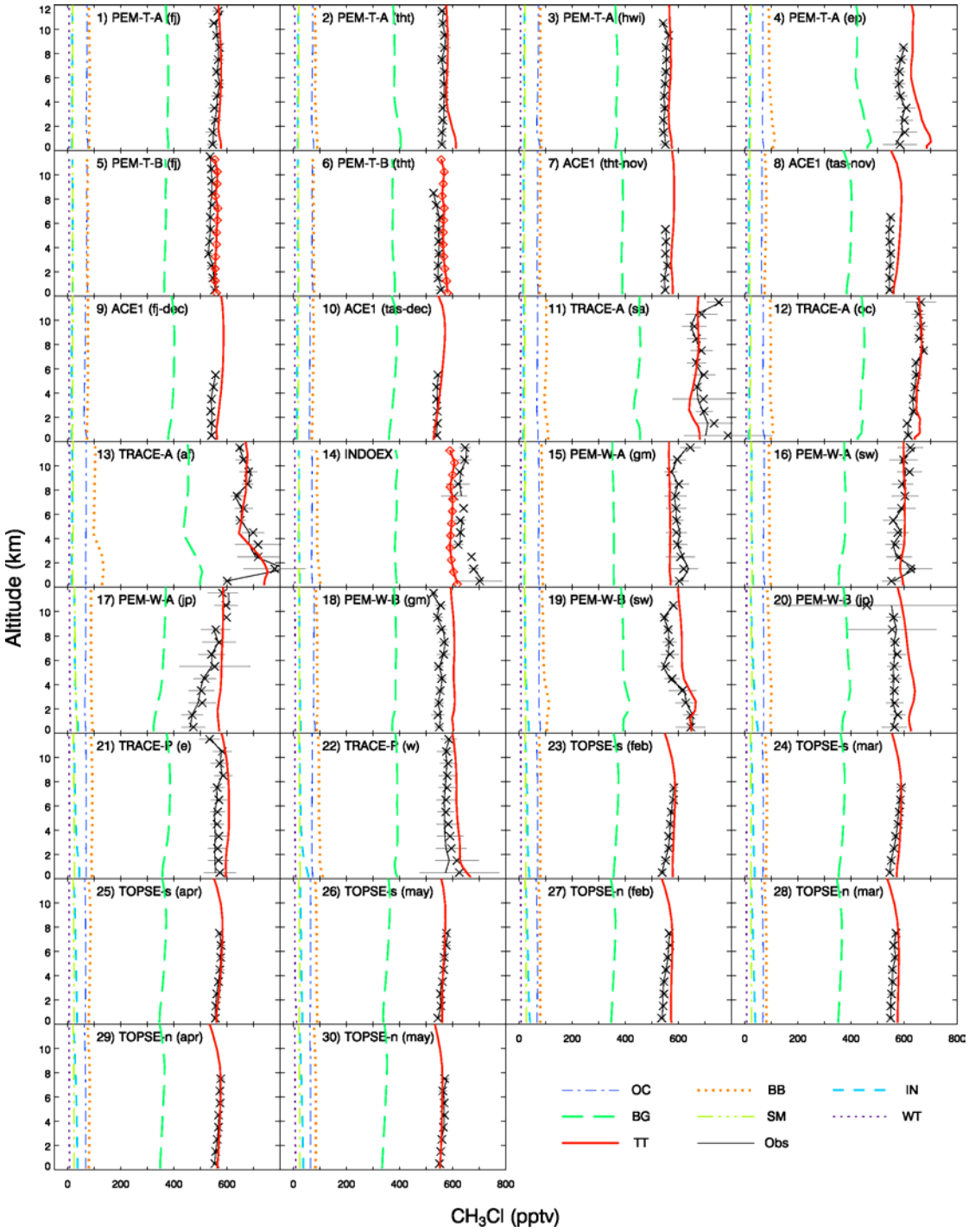

Figure 7. Vertical profiles of CH_3Cl averaged over the aircraft observation regions shown in Figure 4. For the TOPSE experiment, monthly mean values from February to May are calculated. Please see the text for abbreviation for each project region. Thin solid lines indicate the medians of observations, crosses indicate the means of observations, and thin horizontal lines indicate the observed standard deviations. Diamonds indicate the means of the six model runs. For model results, contributions from each source as well as all sources are shown. OC, BB, IN, BG, SM, WT, and TT denote ocean, biomass burning, incineration/industrial, biogenic, salt marshes, wetlands, and total, respectively.

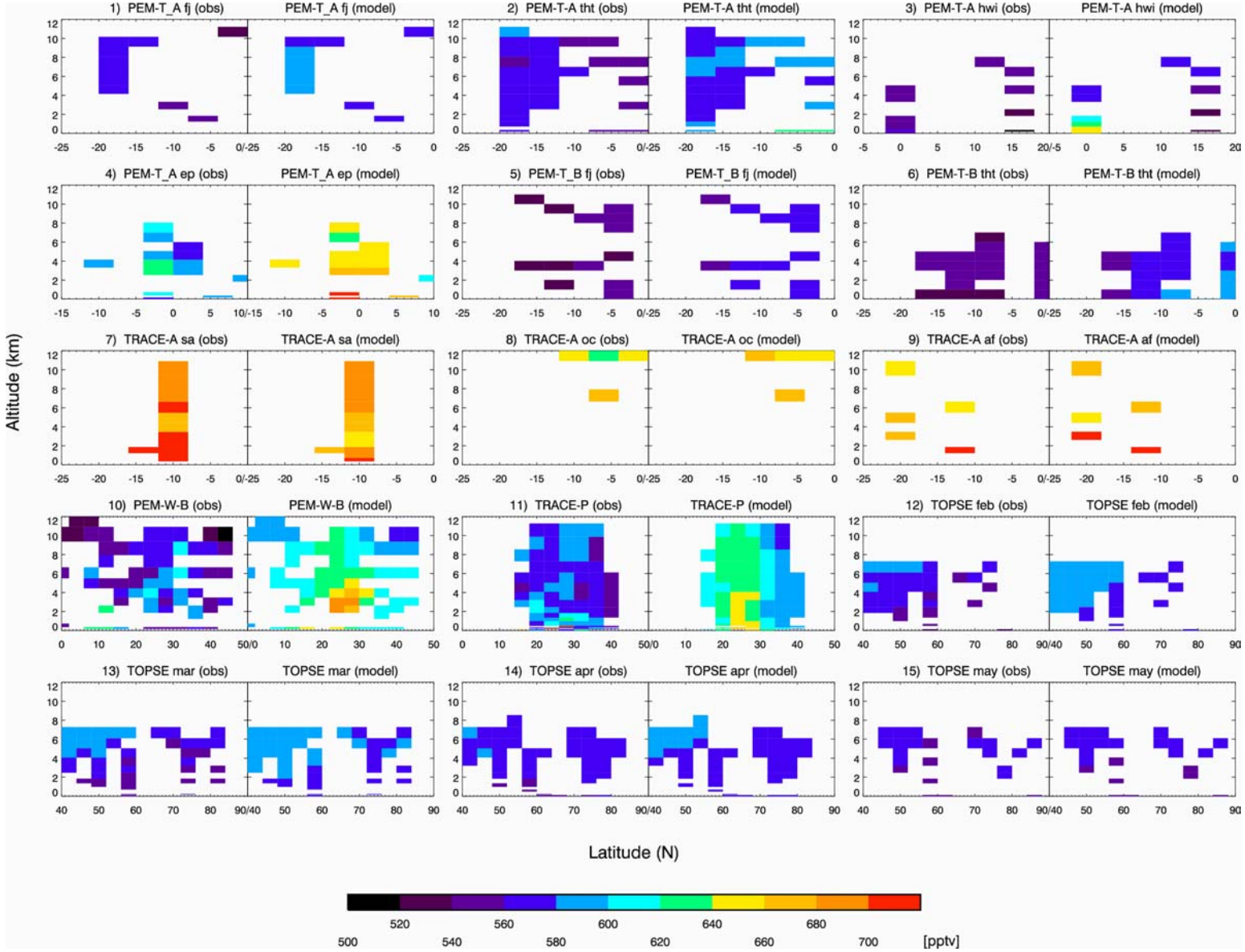

Figure 8. Observed and simulated latitude-altitude distributions for selected aircraft observation regions shown in Figure 4. For TRACE-P and TOPSE, the western/eastern and the northern/southern regions are combined, respectively. Abbreviations are the same as used in Figure 7. Only grid boxes with > 10 observation points are shown.

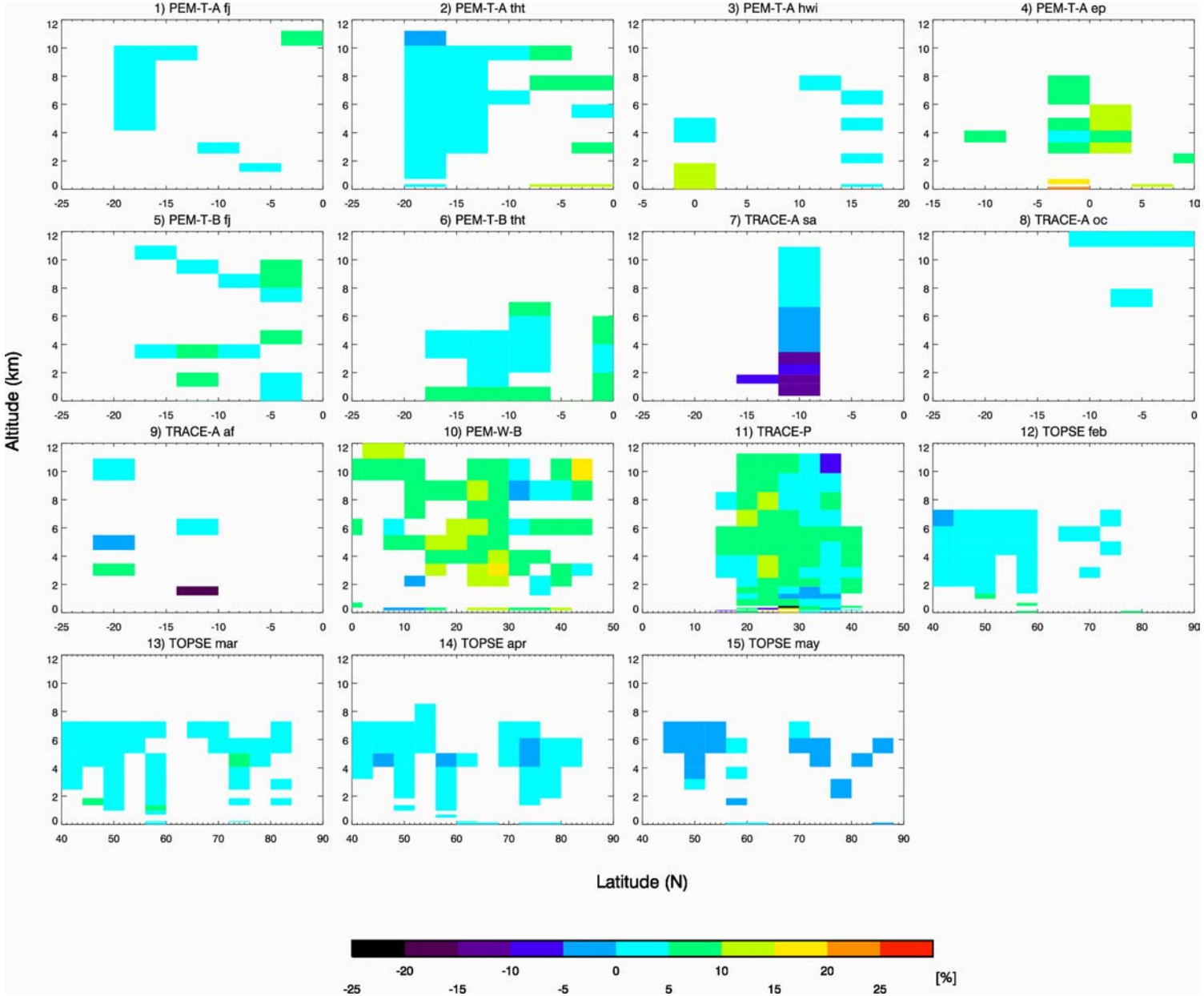

Figure 9. Same as Figure 8 but for the relative difference computed as (model-observation)/model.